CHALMERS
UNIVERSITY OF TECHNOLOGY

The RoboPol sample of optical polarimetric standards

A&A, 677, A144 (2023)
https://doi.org/10.1051/0004-6361/202346778

Astronomy & Astrophysics

The RoboPol sample of optical polarimetric standards*

D. Blinov[1,2], S. Maharana[3,1,4], F. Bouzelou[2], C. Casadio[1,2], E. Gjerløw[5], J. Jormanainen[6,7], S. Kiehlmann[1,2], J. A. Kypriotakis[2,1], I. Liodakis[6], N. Mandarakas[2,1], L. Markopoulioti[2], G. V. Panopoulou[8], V. Pelgrims[1,2], A. Pouliasi[9], S. Romanopoulos[2,1], R. Skalidis[10,1], R. M. Anche[11,3], E. Angelakis[12], J. Antoniadis[1,2], B. J. Medhi[13], T. Hovatta[6], A. Kus[14], N. Kylafis[1,2], A. Mahabal[15], I. Myserlis[16,17], E. Paleologou[1,2], I. Papadakis[1,2], V. Pavlidou[1,2], I. Papamastorakis[1,2], T. J. Pearson[10], S. B. Potter[3,18], A. N. Ramaprakash[4,1,15], A. C. S. Readhead[10], P. Reig[1,2], A. Słowikowska[19,14], K. Tassis[1,2], and J. A. Zensus[17]

[1] Institute of Astrophysics, Foundation for Research and Technology-Hellas, N. Plastira 100, Vassilika Vouton, 71110 Heraklion, Greece
e-mail: blinov@ia.forth.gr
[2] Department of Physics, and Institute for Theoretical and Computational Physics, University of Crete, Voutes University campus, 70013 Heraklion, Greece
[3] South African Astronomical Observatory, PO Box 9, Observatory, 7935 Cape Town, South Africa
[4] Inter-University Centre for Astronomy and Astrophysics, Post Bag 4, Ganeshkhind, Pune-411007, India
[5] Institute of Theoretical Astrophysics, University of Oslo, PO Box 1029 Blindern, 0315 Oslo, Norway
[6] Finnish Centre for Astronomy with ESO, FINCA, University of Turku, Quantum, Vesilinnantie 5, 20014 Turku, Finland
[7] Department of Physics and Astronomy, University of Turku, 20014 Turku, Finland
[8] Department of Space, Earth and Environment, Chalmers University of Technology, Gothenburg, Sweden
[9] University of California, Los Angeles, Geophysics and Space Physics Department of Earth, Planetary, and Space Sciences, Los Angeles, USA
[10] Owens Valley Radio Observatory, California Institute of Technology, MC 249-17, Pasadena, CA 91125, USA
[11] Department of Astronomy/Steward Observatory, Tucson, AZ 85721-0065, USA
[12] Section of Astrophysics, Astronomy & Mechanics, Department of Physics, National and Kapodistrian University of Athens, Panepistimiopolis Zografos 15784, Greece
[13] Department of Physics, Gauhati University, Guwahati-781014, Assam, India
[14] Institute of Astronomy, Faculty of Physics, Astronomy and Informatics, Nicolaus Copernicus University in Toruń, Grudziadzka 5, 87-100 Toruń, Poland
[15] Cahill Center for Astronomy and Astrophysics, California Institute of Technology, 1200 E California Blvd, MC 249-17, Pasadena, CA 91125, USA
[16] Institut de Radioastronomie Millimétrique, Avenida Divina Pastora 7, Local 20, 18012 Granada, Spain
[17] Max-Planck-Institut für Radioastronomie, Auf dem Hügel 69, 53121 Bonn, Germany
[18] Department of Physics, University of Johannesburg, PO Box 524, Auckland Park 2006, South Africa
[19] Joint Institute for VLBI ERIC, Oude Hoogevceensedijk 4, 7991 PD Dwingeloo, The Netherlands

Received 29 April 2023 / Accepted 19 July 2023

ABSTRACT

Context. Optical polarimeters are typically calibrated using measurements of stars with known and stable polarization parameters. However, there is a lack of such stars available across the sky. Many of the currently available standards are not suitable for medium and large telescopes due to their high brightness. Moreover, as we find, some of the polarimetric standards used are in fact variable or have polarization parameters that differ from their cataloged values.
Aims. Our goal is to establish a sample of stable standards suitable for calibrating linear optical polarimeters with an accuracy down to 10^{-3} in fractional polarization.
Methods. For 4 yr, we have been running a monitoring campaign of a sample of standard candidates comprised of 107 stars distributed across the northern sky. We analyzed the variability of the linear polarization of these stars, taking into account the non-Gaussian nature of fractional polarization measurements. For a subsample of nine stars, we also performed multiband polarization measurements.
Results. We created a new catalog of 65 stars (see Table 2) that are stable, have small uncertainties of measured polarimetric parameters, and can be used as calibrators of polarimeters at medium and large telescopes.

Key words. polarization – techniques: polarimetric – standards

1. Introduction

Polarimetry, on its own and in combination with other techniques, is a powerful tool for probing the physical conditions of astrophysical sources. Like all experimental techniques, polarimetric observations require careful calibration and control of instrumental systematics. In the case of optical polarimetry, standard stars with known polarization properties are used for calibration purposes. Unfortunately, the number of reliable polarimetric standards is very limited. There are fewer than 30 stars in the two hemispheres with polarization degree (PD)

* All data discussed in this paper are available in Harvard Dataverse at https://doi.org/10.7910/DVN/IV9TXX.

known to an accuracy of 0.1% or better, and proven to be stable in time (e.g., Schmidt et al. 1992; Hsu & Breger 1982). The lack of an appropriate unpolarized standard star in the night sky at a given moment is common.

The situation is particularly difficult for telescopes with apertures larger than 1m. They often have a lower limit on the brightness of sources suitable for observations due to CCD saturation constraints. Meanwhile, most unpolarized standards are very bright ($<8^m$), making them unsuitable for calibration on such telescopes because unpolarized standards are selected from nearby stars to ensure that their light does not pass through a significant column of dust in the interstellar medium.

Another problem is the lack of polarized standards with low, but not negligible, PD in the range between 0.1 and 2%. Existing measurements of standards with PD > 2% have been sufficient to calibrate conventional polarimeters, and there has been no need for covering a lower range of PD. It is because conventional polarimeters have (or are assumed to have) negligible crosstalk between the Stokes parameters, meaning that the parameters are independent and uncorrelated. In this case we use unpolarized stars (zero-polarized or negligibly polarized) to find the offset of the instrumental Q/I–U/I plane with respect to the standard value and (2) highly polarized stars to find a rotation of the instrumental relative Stokes parameters plane with respect to the standard value (e.g., Ramaprakash et al. 2019). However, some new polarimeters have significant crosstalk (Tinbergen 2007; Wiersema et al. 2018; Maharana et al. 2022; Wiktorowicz et al. 2023). This crosstalk must be modeled in the entire range of PDs of interest, including the 0.1 to 2% range (the level of interstellar medium-induced stellar polarization in the diffuse interstellar medium). The lack of standards covering a range of polarization values hinders efficient calibration of modern polarimeters where crosstalk between the relative Stokes Q/I and U/I parameters is significant.

Finally, a significant fraction of stars that are widely recognized as reliable standards exhibit inconsistent polarization parameters across different sources in the literature, and in some cases, they have been found to be variable (see, e.g., Table 1). A few examples of such studies follow. Hsu & Breger (1982), after monitoring 12 previously used standards, found that 3 of them were variable. Dolan & Tapia (1986) also questioned the stability of three standards. Bastien et al. (1988) monitored 13 previously known polarized standard stars and found 11 of them to be variable. Their methods were criticized by Clarke & Naghizadeh-Khouei (1994). However, after considering this criticism and applying more rigorous statistical methods, Bastien et al. (2007) reached a very similar conclusion: out of these 13 standards, 7 show significant variability, while 4 others may also be variable. In a study by Clemens & Tapia (1990), a single-epoch survey of 16 stars previously used as polarization standards was conducted. The study found that four of these stars had significantly different polarization parameters compared to the previously published values. Breus et al. (2021) found that nine stars used as calibrators in previous studies show variability. As another example, while performing our polarimetric monitoring program, RoboPol[1], we found that VI Cyg 12 (also known as Cyg OB2 #12 or Schulte 12), which is used as a highly polarized standard in many observatories, is variable in polarization (see Fig. 1). Indeed, VI Cyg 12 has been shown to be a luminous blue variable with a circumstellar dust shell (Chentsov et al. 2013). The standard deviation of the electric vector position angle (EVPA) in our measurements of this star is >0.8°. Therefore, it should not be used for calibration if the desired accuracy of EVPA zero point calibration is stricter. Based on RoboPol monitoring data, BD+33.2642 is suspected to have different polarization values than previously reported (Skalidis et al. 2018).

There have been recent attempts to revise the parameters of polarization standards in use or to establish new samples of calibrators. Breus et al. (2021) report on their observations of a large sample (~100 stars) that had been considered as calibrators in various studies and offer revised and/or refined values of the polarization parameters of these stars. Gil-Hutton & Benavidez (2003) proposed a sample of nearby low-polarization stars in the southern hemisphere. Additionally, stars in the solar vicinity with measured polarization parameters obtained for the interstellar medium (e.g., Piirola et al. 2020) and white dwarf physics (Żejmo et al. 2017) studies can be used as unpolarized standards. Nevertheless, all candidate standard stars provided in these works are subject to one or several of the above-mentioned deficiencies. They are either very bright or they have not been proven to be stable (i.e., is measured only a few times or measured multiple times over a very short time interval).

In summary, there is a long-standing need in the optical polarimetry community to establish a large homogeneous list of polarimetric standards that will facilitate characterization of instrument performance. The aim of this work is to contribute in this direction.

2. Sample of polarization-standard candidates

To meet the challenges of establishing a large set of reliable polarization standards, we selected an initial sample of 121 candidate stars, which was made up of four independent subsamples. They are described below.

Sample B, 35 polarized stars ($\mathrm{PD}/\sigma_{\mathrm{PD}} \geq 3$) in fields of blazars monitored within the RoboPol program that did not show any significant variability between 2013 and 2016: RoboPol is a linear optical polarimeter designed for efficient monitoring of point sources such as blazars or stars (see Sect. 3.1 and Ramaprakash et al. 2019). The point sources are placed in a central 22 × 22 arcsec masked area, where the sky background is reduced. However, the polarimeter also has a large unmasked field of view (FoV) of 13 × 13 arcmin, which allows linear polarimetry of all sources in the field, but with higher noise compared to the central target. High-cadence polarimetric monitoring of about 100 blazars was performed between 2013 and 2016 (Blinov et al. 2021). Most of the sources were observed several tens to a few hundred times. This provided the same number of observations of stars in the corresponding fields. We analyzed the field stars data and selected 35 sources from these fields that showed stable polarization (see Sect. 4) throughout the monitoring period.

Sample H, 6 stars selected from the Heiles (2000) catalog, with brightness in the range $8^m < R < 14^m$: Three are highly polarized stars. Three more have low polarization and fill the range in right ascension (RA), where there is a lack of low-polarization stars in other samples.

Sample L, 54 photometric standard stars distributed along the celestial equator from Landolt (1992): To select these sources we used an atlas of Landolt standards compiled by P. S. Smith[2]. The selection criteria of stars in this atlas were (1) declination (Dec) $\delta > -20°$; (2) observed by Landolt (1992) on at least five

[1] http://robopol.org

[2] http://james.as.arizona.edu/~psmith/61inch/ATLAS/atlasinfo.html

Table 1. Polarization parameters of standard stars monitored by RoboPol, as reported in the literature.

Source	RA	Dec	Band	PD (%)	EVPA (°)	References
			polarized			
BD+57.2615	22:47:49.6	+58:08:50	*R*	2.02 ± 0.05	41.0 ± 1.0	Whittet et al. (1992)
BD+59.389[(c)]	02:02:42.1	+60:15:26	*R*	6.430 ± 0.022	98.14 ± 0.10	Schmidt et al. (1992)
BD+64.106	00:57:36.7	+64:51:35	*R*	5.150 ± 0.098	96.74 ± 0.54	Schmidt et al. (1992)
CMaR1 24	07:04:47.4	−10:56:18	*R*	3.18 ± 0.09	86.0 ± 1.0	Whittet et al. (1992)
CygOB2 14	20:32:16.6	+41:25:36	*R*	3.13 ± 0.05	86.0 ± 1.0	Whittet et al. (1992)
HD147283	16:21:57.7	−24:29:44	*R*	1.59 ± 0.03	174.0 ± 1.0[(*)]	Whittet et al. (1992)
	−〃−	−〃−	*R*	1.81	176.0	Carrasco et al. (1973)
HD147343	16:22:19.9	−24:21:48	*R*	0.43 ± 0.05	151.0 ± 3.0	Whittet et al. (1992)
HD150193	16:40:17.9	−23:53:45	*R*	5.19 ± 0.05	56.0 ± 1.0	Whittet et al. (1992)
HD154445[(c)]	17:05:32.3	−00:53:31	*R*	3.683 ± 0.072	88.91 ± 0.56	Schmidt et al. (1992)
	−〃−	−〃−	*R*	3.63 ± 0.01	90.0 ± 0.1[(*)]	Hsu & Breger (1982)
HD155197[(c)]	17:10:15.8	−04:50:04	*R*	4.274 ± 0.027	102.88 ± 0.18	Schmidt et al. (1992)
HD161056	17:43:47.0	−07:04:47	*R*	4.012 ± 0.032	67.33 ± 0.23	Schmidt et al. (1992)
HD183143[(b,c)]	19:27:26.6	+18:17:45	*R*	5.90 ± 0.05	179.2 ± 0.2[(*)]	Hsu & Breger (1982)
	−〃−	−〃−	*R*	5.7 ± 0.04	178.0 ± 1.0	Bailey & Hough (1982)
HD204827[(b,c)]	21:28:57.8	+58:44:23	*R*	4.893 ± 0.029	59.10 ± 0.17[(*)]	Schmidt et al. (1992)
	−〃−	−〃−	*R*	4.86 ± 0.05	60.0 ± 1.0	Bailey & Hough (1982)
	−〃−	−〃−	*R*	4.99 ± 0.05	59.9 ± 0.1	Hsu & Breger (1982)
HD215806	22:46:40.2	+58:17:44	*R*	1.83 ± 0.04	66.0 ± 1.0	Whittet et al. (1992)
HD236633	01:09:12.3	+60:37:41	*R*	5.376 ± 0.028	93.04 ± 0.15	Schmidt et al. (1992)
Hiltner960[(a)]	20:23:28.5	+39:20:59	*R*	5.210 ± 0.029	54.54 ± 0.16	Schmidt et al. (1992)
VICyg12[(b)]	20:32:41.0	+41:14:29	*R*	7.97 ± 0.05	117.0 ± 1.0	Whittet et al. (1992)
	−〃−	−〃−	*R*	7.893 ± 0.037	116.23 ± 0.14[(*)]	Schmidt et al. (1992)
	−〃−	−〃−	*R*	7.18 ± 0.04	117.0 ± 1.0	Hsu & Breger (1982)
			unpolarized			
BD+28.4211	21:51:11.0	+28:51:50	*V*	0.054 ± 0.027	54.22	Schmidt et al. (1992)
BD+32.3739[(c)]	20:12:02.1	+32:47:44	*V*	0.025 ± 0.017	35.79	Schmidt et al. (1992)
BD+33.2642	15:51:59.9	+32:56:54	*R*	0.20 ± 0.15	78 ± 20	Skalidis et al. (2018)
BD+40.2704	13:54:07.2	+39:37:59	?	0.07 ± 0.02	57 ± 9	Berdyugin & Teerikorpi (2002)
G191B2B	05:05:30.6	+52:49:52	*V*	0.061 ± 0.038	147.65	Schmidt et al. (1992)
HD14069	02:16:45.2	+07:41:11	*V*	0.022 ± 0.019	156.57	Schmidt et al. (1992)
HD154892	17:07:41.3	+15:12:38	*B*	0.05 ± 0.03	–	Turnshek et al. (1990)
HD212311[(c)]	22:21:58.6	+56:31:53	*V*	0.034 ± 0.021	50.99	Schmidt et al. (1992)
HD21447	03:30:00.2	+55:27:07	*V*	0.051 ± 0.020	171.49	Schmidt et al. (1992)
HD94851	10:56:44.3	−20:39:53	*B*	0.057 ± 0.018	–	Turnshek et al. (1990)
WD2149+021	21:52:25.4	+02:23:20	*R*	0.050 ± 0.006	−63 ± 3	Cikota et al. (2017)

Notes. [(a)]Possibly variable You et al. (2017); [(b)]variable in RoboPol data and/or in Hsu & Breger (1982); Dolan & Tapia (1986); [(c)]possibly variable Breus et al. (2021). For stars with multiple literature values, [(*)]flags the value used for the EVPA zero point calibration in Sect. 3.1.

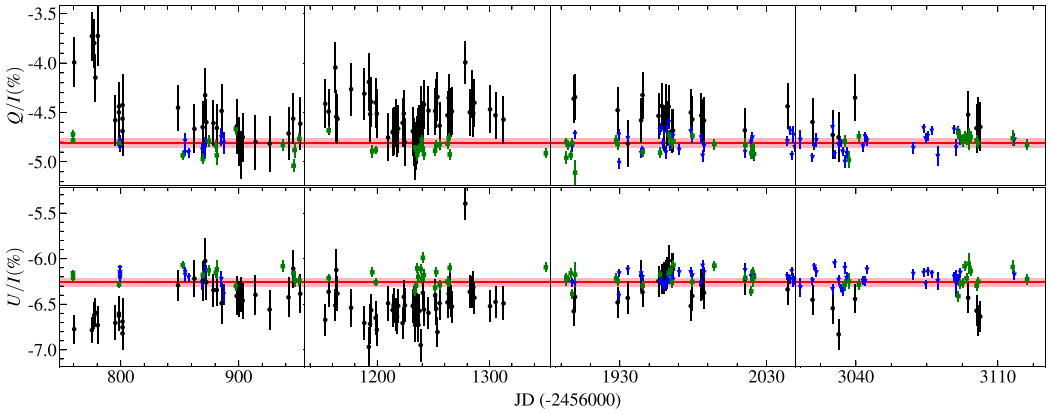

Fig. 1. *R*-band relative Stokes parameters of VI Cyg 12 (black circles) in comparison with two other standards: BD+32.3739 (blue triangles) and HD 212311 (green squares). The horizontal red lines and the pink areas represent Q/I and U/I values for VI Cyg 12 from Schmidt et al. (1992) with corresponding uncertainties. For ease of visualization, the values for the two other stars are shifted so that their average Stokes parameters match the red line. In spite of larger photon noise uncertainties, it is clear that the Stokes parameters of VI Cyg 12 are significantly variable and systematically deviate from their catalog values during long periods of time.

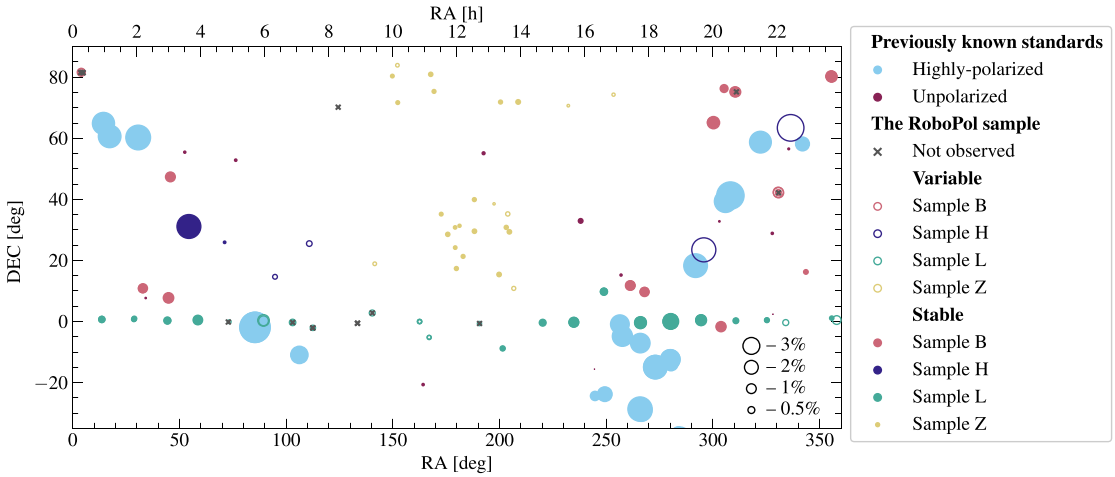

Fig. 2. Distribution of the sample stars over the sky. Samples B, H, L, and Z are described in Sect. 2. Fourteen stars marked as "not observed" and that have zero measurements were excluded from the final sample. Highly polarized and unpolarized stars are standards used in the previous studies listed in Table 1. The symbol size indicates polarization of individual stars from Table A.4.

nights; and (3) absence of confirmed or suspected variability. The atlas stars are distributed in 6.8×6.8 arcmin fields every 1 h in RA near Dec = 0°. We selected 2 to 4 stars in each field, with brightness in the range $8^m < R < 14^m$.

Sample Z: 26 unpolarized stars at high Galactic latitudes, from a single epoch survey by Berdyugin et al. (2014) that have fractional polarization PD < 0.1%, with uncertainties σ_{PD} < 0.05%.

The properties of the selected standard-star candidates are summarized in Table A.1, where Star ID prefixes correspond to one of the four samples. The advantages of our sample are that it is widely distributed over the northern sky (see Fig. 2) and partially available from the southern hemisphere. It contains relatively faint stars that are accessible to medium and large telescopes. Moreover, a significant fraction of the sample are Landolt stars. Therefore, they can be used for simultaneous polarimetric and absolute photometric calibration of instruments (i.e., I, Q, and U Stokes parameters can be calibrated together).

3. Observations and data reduction

We monitored the linear polarization parameters of the sample of candidate stars for four consecutive years in order to confirm their stability. The monitoring was performed using the RoboPol polarimeter. Additionally, we performed single-epoch measurements of a small subsample using the Nordic Optical Telescope. These observations are described in the following subsections.

3.1. RoboPol monitoring and data reduction

We carried out our polarimetric monitoring of the selected sample in the Cousins R-band and SDSS r'-band from May 2017 to June 2021 using the RoboPol polarimeter at the 1.3 m telescope of the Skinakas observatory. Every year observations are performed from May to November. Because the observatory does not operate during winter months, sources around RA = 12 h were insufficiently sampled. Of the initial 121 stars selected for monitoring, 14 were never observed or have poor quality of measurements. For this reason, they were dropped from the sample. However, most of them were located near other stars in the sample, and therefore would not increase much the sky coverage of our final standards catalog.

The polarizing assembly of the polarimeter consists of two half-wave plates and two Wollaston prisms aligned in such a way that any incident ray is split into four rays or channels with the polarization state rotated by 45° with respect to each other. RoboPol has no moving parts except the filter wheel, which simplifies operations and instrumental polarization modeling. Three Stokes parameters $q = Q/I$, $u = U/I$, and I (the last only when stars with known magnitude are present in the 13×13 arcmin FoV) can be measured simultaneously with a single exposure. The optical and mechanical design of RoboPol is described in Ramaprakash et al. (2019). All data for this program were collected in the central masked region of the FoV where systematic uncertainties are <0.1% (Ramaprakash et al. 2019).

The data were processed using the standard RoboPol pipeline, which is described by King et al. (2014), with modifications presented by Blinov et al. (2021). Further corrections were introduced at the calibration stage using known standard stars measurements. The details of this process are described below.

Standard processing of RoboPol data includes an instrumental polarization correction model. This model was created based on combined measurements obtained during multiple years of several unpolarized standard stars in a grid of hundreds of positions uniformly covering the FoV (King et al. 2014). Therefore, it approximates well the large-scale instrumental polarization variation across the entire FoV. However, we discovered that for stars measured in the central masked area there is a residual instrumental polarization that is unaccounted for by the model, and that depends on the (x, y) source position on the CCD. In Fig. 3 we show an example of such subtle instrumental polarization changes for unpolarized standards measured in 2019. A clear position-dependent trend with an amplitude of ~0.5% in the measured values of relative Stokes parameters can be seen. Since all measurements discussed in this work were observed in the central masked area, we had to correct them for this trend. We approximated these $q(x, y) = \frac{Q}{I}(x, y)$ and $u(x, y) = \frac{U}{I}(x, y)$ dependences with a quadratic surface for each observing season separately. Using these fits, we corrected all measurements of corresponding seasons. Then, we determined the standard deviations in the q and u estimates for the unpolarized standards, and propagated these values with the corresponding uncertainties of standard candidates measurements.

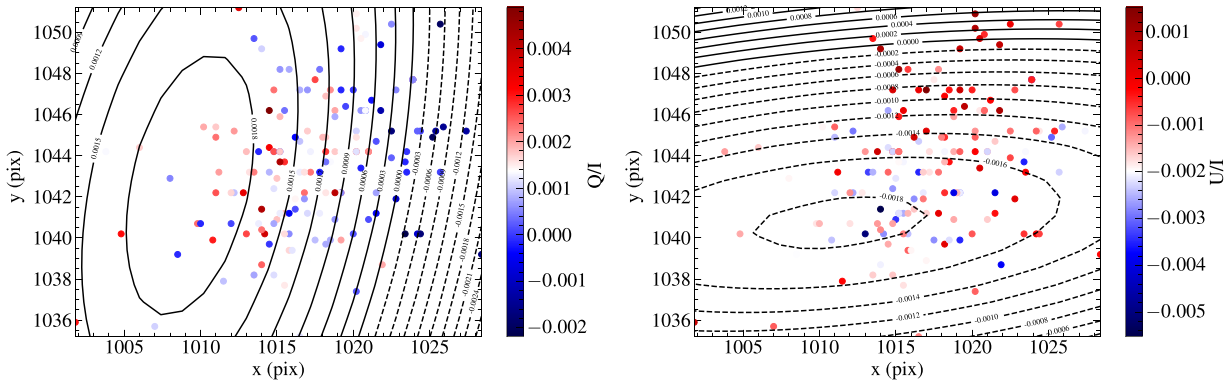

Fig. 3. Relative Stokes parameters of zero-polarization standards from Table 1 observed in 2019 in the central masked area as a function of the position on the CCD. The color of the points indicates the deviation of Q/I or U/I from zero (see color bars). The planar contours show the fitted quadratic surface.

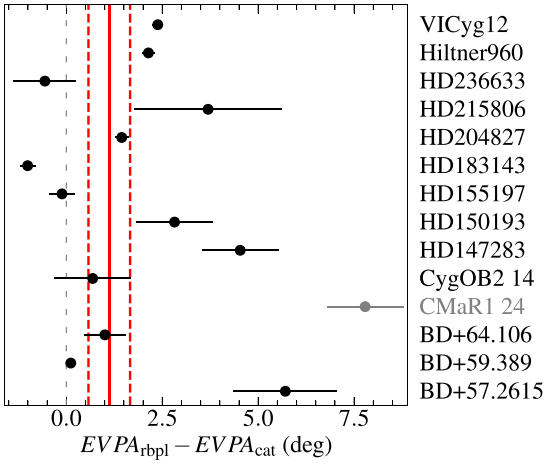

Fig. 4. Differences between weighted average of observed EVPA and corresponding catalog values for the 14 most reliable highly polarized standards. Weighted mean value for 13 stars (CMaR1 24 is excluded by 3σ-clipping) is shown by the solid red line, while the standard error of the mean is shown by the red dashed lines.

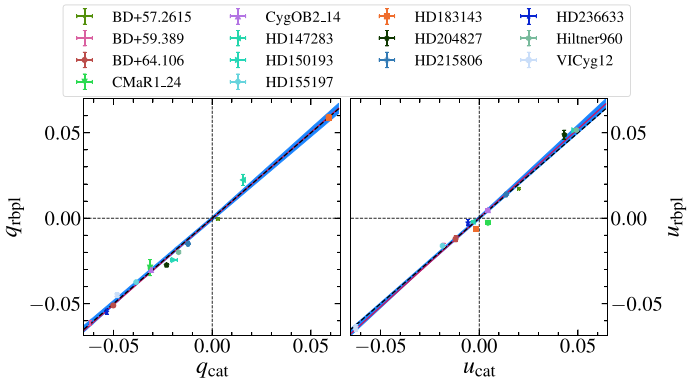

Fig. 5. Weighted mean values of Stokes parameters of high-polarization standards, as measured by RoboPol vs. catalog values from Table 1. The black dashed line is $y = x$; the red solid line is the ordinary least-squares regression fit to the data. The light blue region is the 1σ uncertainty region of the fit.

We found the rotation of the instrumental q–u plane with respect to the standard reference frame using highly polarized standards (Table 1) that were monitored along with the standard candidates sample. Since individual catalog values for these standards are unreliable (see Sect. 1), we used a statistical approach: the entire sample was considered, including stars that are known to be variable (e.g., VI Cyg 12). For each standard we computed the weighted mean of the relative Stokes parameters combining all measurements along the observing period. Then, using these q, u estimates, we calculated the corresponding $EVPA_{rbpl}$ values of each star in our measurements, and found the difference between this value and that reported in the literature, $EVPA_{cat}$. For stars with multiple values reported in the literature, we used either the value with the smallest uncertainty, or the most recent measurement if the uncertainties are comparable. The $EVPA_{cat}$ values used are flagged with asterisks in Table 1. The corresponding differences between the RoboPol and literature estimates are shown in Fig. 4. We found the weighted mean of $EVPA_{rbpl} - EVPA_{cat}$ to be $1.1 \pm 0.5°$, after applying 3σ-clipping, which excluded *CMaR1 24* from the averaging. This value was used as the instrumental EVPA zero-point correction, and all measurements were adjusted for it, while uncertainties were propagated accordingly.

We assessed the possibility that the polarimeter has a crosstalk between the relative Stokes parameters by measuring their covariance. We first corrected the measurements of unpolarized standards for the polarization and EVPA zero points as described before. Then, we calculated the correlation coefficient between q and u for each individual standard. There was no significant systematic correlation found among stars. We also calculated the correlation coefficient r for a set of standard star measurements for each season. In all cases $|r|$ does not exceed 0.42, while the median value among seasons is $r = -0.17$. Therefore, we conclude that the crosstalk between channels of the polarimeter is negligible with respect to the noise level.

We also verified that the polarimetric efficiency of the instrument is 100% within measurement errors (i.e., the measured polarimetric accuracy is independent of the source polarization). To this end, we corrected the Stokes parameters of the highly polarized stars for the zero points, and then compared them with the corresponding literature values. The orthogonal distance regression fits to the data are consistent with the expected $q_{rbpl} = q_{cat}$ and $u_{rbpl} = u_{cat}$ dependences within 1σ, as shown in Fig. 5.

3.2. NOT observations and data analysis

We selected a subset of ten standard candidates based on visibility, limited available observing time for this program, and

preliminary stability observed in the RoboPol data. Subsequently, we conducted observations of these candidates using the Nordic Optical Telescope (NOT) under proposal 61-608. The Alhambra Faint Object Spectrograph and Camera (ALFOSC) instrument[3] was used in its polarimetric mode. It is a two-channel polarimeter consisting of a rotating half-wave plate (HWP) and a calcite plate. For each object, two beam images called o and e are formed, corresponding to the 0° and 90° polarizations coming out of the WP, respectively. Standard candidates were observed with sequences consisting of eight exposures, corresponding to HWP positions of 0° to 180° in steps of 22.5°. This yields four Q/I and U/I measurements for each star. Observations were performed during the nights of 8 and 23 September and 13 December 2020 in multiple filters. Most of the stars were observed in SDSS g-, r-, and i-bands and Johnson-Cousins B-, V-, and R-bands, while two stars were also observed in the U-band. Unpolarized standard stars BD+28.4211, HD 212311, and highly polarized standards Hiltner 960, VI Cyg 12, BD+59.389, BD+64.106, HD 204827 were observed during the same nights as the program targets. These standards were observed with sequences consisting of 16 exposures corresponding to HWP positions of 0° to 360° in steps of 22.5°. This provided eight Q/I and U/I measurements for each star.

For the analysis of the raw data, we developed a semi-automated data reduction pipeline in Python. Attention was paid to error estimation and propagation in each step of the analysis. Photometry was done using the aperture photometry package of the Photutils library[4]. To find the polarization parameters, we followed the procedure from Patat & Romaniello (2006). For each HWP position $\{\theta_i = i \times 22.5^\circ \mid i \in \{0, 1, ..., N\}\}$ we calculated the normalized flux differences between the o and e star images:

$$F_i = \frac{f_{o,i} - f_{e,i}}{f_{o,i} + f_{e,i}}. \tag{1}$$

Then the relative Stokes parameters were expressed as

$$q \equiv \frac{Q}{I} = \frac{2}{N}\sum_{i=0}^{N-1} F_i \cos\left(\frac{\pi}{2}i\right), \tag{2}$$

$$u \equiv \frac{U}{I} = \frac{2}{N}\sum_{i=0}^{N-1} F_i \sin\left(\frac{\pi}{2}i\right). \tag{3}$$

Using these q and u estimates, we inferred PD and EVPA, and their uncertainties as described in Sect. 3.3. Then we examined dependences of the PD and EVPA estimates on the photometry aperture radius, and selected optimal aperture and annulus radii, where both parameters reach a plateau and minimal uncertainties. The same procedure was performed for the observations of the standard stars. Using their polarization parameters, we found the instrumental polarization and EVPA zero points in each band individually. However, in the U-band, no standards were observed either during our observations or during adjacent nights. In the SDSS g- and r-bands, only a single standard star measurement (BD+28.4211) was available. Therefore, we fitted the dependences of the instrumental q and u on the effective wavelength using all other bands with a linear function. By utilizing these fits, we determined the instrumental zero points of the relative Stokes parameters in each band and applied corrections to all measurements based on these values.

[3] http://www.not.iac.es/instruments/alfosc/
[4] https://photutils.readthedocs.io/en/stable/

3.3. Polarization parameter estimates and their uncertainties

The polarization degree and its uncertainty were calculated assuming that the relative Stokes parameters $q = Q/I$ and $u = U/I$ follow a normal distribution:

$$\mathrm{PD} = \sqrt{q^2 + u^2}, \quad \sigma_{\mathrm{PD}} = \sqrt{\frac{q^2\sigma_{\mathrm{q}}^2 + u^2\sigma_{\mathrm{u}}^2}{q^2 + u^2}}. \tag{4}$$

Any linear polarization measurement is biased towards higher PD values (Serkowski 1958). The PD follows a Rician distribution (Rice 1945) and significantly deviates from the normal distribution at low signal-to-noise ratios. There are a variety of methods suggested for correction of this bias (e.g., Simmons & Stewart 1985; Vaillancourt 2006). Our catalog provides the flexibility to select any debiasing method as the relative Stokes parameters constitute our ultimate data product. The data presented in this paper remain uncorrected for polarization bias. The relative Stokes parameters themselves are unbiased quantities.

The EVPA is defined as

$$\mathrm{EVPA} = \frac{1}{2}\,\mathrm{atan2}\left(\frac{u}{q}\right) \equiv \begin{cases} \arctan\left(\frac{u}{q}\right) & q > 0 \\ \arctan\left(\frac{u}{q}\right) + \pi & u \geq 0,\ q < 0 \\ \arctan\left(\frac{u}{q}\right) - \pi & u < 0,\ q < 0 \\ \frac{\pi}{2} & u > 0,\ q = 0 \\ -\frac{\pi}{2} & u < 0,\ q = 0 \\ \text{undefined} & u = 0,\ q = 0 \end{cases}, \tag{5}$$

while its measurements are also non-Gaussian and defined by the following probability density (Naghizadeh-Khouei & Clarke 1993):

$$G(\theta; \theta_o; \mathrm{PD}_o) = \frac{1}{\sqrt{\pi}}\left\{\frac{1}{\sqrt{\pi}} + \eta_o e^{\eta_o^2}[1 + \mathrm{erf}(\eta_o)]\right\}\exp\left(-\frac{\mathrm{PD}_o^2}{2\sigma_{\mathrm{PD}}^2}\right). \tag{6}$$

Here $\eta_o = \mathrm{PD}_o \cos 2(\theta - \theta_o)/(\sigma_{\mathrm{PD}}\sqrt{2})$, erf is the Gaussian error function, PD_o and θ_o are the true values of PD and EVPA, and σ_{PD} is the uncertainty of PD[5].

We determine the EVPA uncertainty σ_θ numerically, by solving the following integral:

$$\int_{-1\sigma_\theta}^{1\sigma_\theta} G(\theta; \mathrm{PD}_o)d\theta = 68.27\%. \tag{7}$$

The true value of PD in this procedure was estimated following Vaillancourt (2006) as

$$\mathrm{PD}_o = \begin{cases} 0 & \text{for } \mathrm{PD}/\sigma_{\mathrm{PD}} < \sqrt{2} \\ \sqrt{\mathrm{PD}^2 - \sigma_{\mathrm{PD}}^2} & \text{for } \mathrm{PD}/\sigma_{\mathrm{PD}} \geq \sqrt{2} \end{cases}. \tag{8}$$

For high S/N values, $\mathrm{PD}/\sigma_{\mathrm{PD}} \geq 20$, the uncertainty of EVPA was approximated as $\sigma_\theta = \mathrm{PD}/(2\sigma_{\mathrm{PD}})$.

[5] The equation for η_o is missing the factor of 2 for the cosine argument in Clarke (2009); the correct formula is provided in Naghizadeh-Khouei & Clarke (1993).

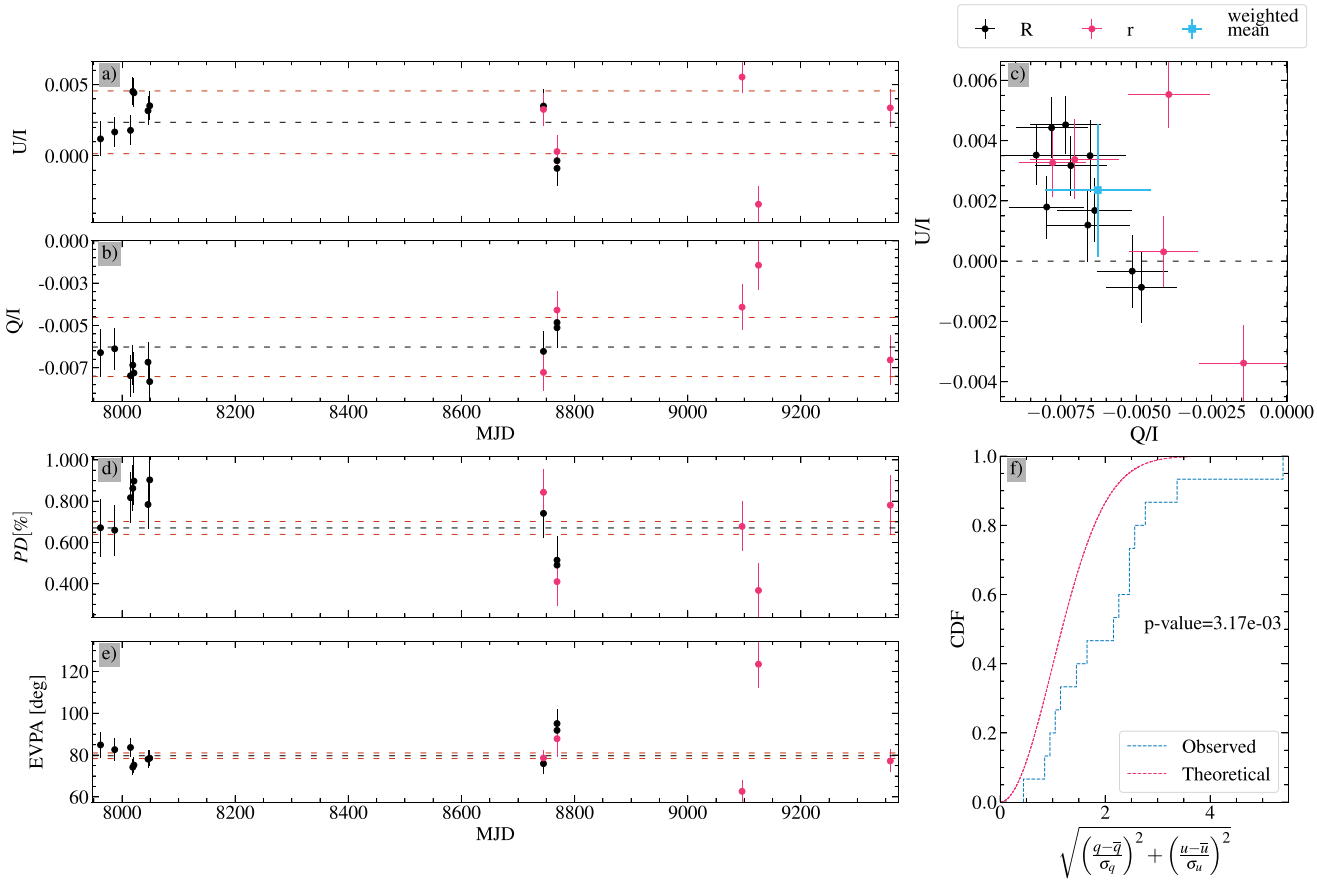

Fig. 6. Evolution of polarization parameters of B_0017+8135_82, which is found to be variable. (a, b) Evolution of the relative Stokes parameters. The dashed black line shows the weighted average; the red dashed lines show the corresponding 1σ uncertainty. (c) Distribution of measurements on the relative Stokes parameters plane. (d, e) Evolution of the polarization degree and the electric vector position angle. The dashed black line shows the weighted average; the red dashed lines show the corresponding 1σ uncertainty. (f) EDF of measured polarization in both bands together with expected CDF of polarization measurements for a constant source with similar uncertainties.

4. Analysis of variability

We assessed the variability of the sample stars following Clarke et al. (1993) and Bastien et al. (2007). The method can be summarized as follows. If the measurements of the relative Stokes parameters q and u are independent and follow normal distributions with means q_0 and u_0, then the statistic

$$\wp = \sqrt{\left(\frac{q}{\sigma_q}\right)^2 + \left(\frac{u}{\sigma_u}\right)^2}, \tag{9}$$

as demonstrated by Simmons & Stewart (1985), follows the Rician distribution (Rice 1945)

$$f(\wp, \wp_0) = \wp \exp\left(-\frac{\wp^2 + \wp_0^2}{2}\right) J_0(i\wp\wp_0), \tag{10}$$

where i is the unit imaginary number, J_0 is the zeroth order Bessel function, and $\wp_0 = \sqrt{(q_0/\sigma_{q0})^2 + (u_0/\sigma_{u0})^2}$. In the case of an unpolarized source ($\wp_0 = 0$), Eq. (10) reduces to the Rayleigh distribution:

$$f(\wp, 0) = \wp \exp\left(-\frac{\wp^2}{2}\right). \tag{11}$$

Then, the cumulative distribution function (CDF) of $\wp$ is expressed as:

$$\mathrm{CDF}(\wp) = \frac{\int_0^{\wp} f(\wp, 0) d\wp}{\int_0^{\infty} f(\wp, 0) d\wp} = 1 - \exp\left(-\frac{\wp^2}{2}\right). \tag{12}$$

In practice, the CDF is approximated by the empirical cumulative distribution function (EDF):

$$\mathrm{EDF}(\wp) = \frac{\text{number of observations} < \wp}{\text{total number of observations}}. \tag{13}$$

The EDF can deviate significantly from the CDF in two cases: (1) the source has variable polarization; (2) the uncertainties σ_q and σ_u are incorrectly estimated. Since in either of these cases the measurements of a star cannot be considered for establishing it as a standard, we do not distinguish between them.

In the case of a polarized source, its weighted means of the measured normalized Stokes parameters $\overline{q}$ and $\overline{u}$ were used as estimates for q_0 and u_0 in order to reduce the polarization to zero:

$$\wp_{\mathrm{reduced}} = \sqrt{\left(\frac{q - \overline{q}}{\sigma_q}\right)^2 + \left(\frac{u - \overline{u}}{\sigma_u}\right)^2}. \tag{14}$$

In order to assess whether the EDF significantly deviates from the CDF of a constant source given by Eq. (12), we used a

Table 2. Average polarization parameters of stable (2σ S.L.) stars in the established sample of standards.

Star ID	RA (J2000) (h:m:s)	Dec (J2000) (°:′:″)	RA(J2000) (°)	Dec(J2000) (°)	Q/I	U/I	Gmag
Low-polarization (PD ≤ 0.5%) stars							
L_92_245	00:54:16.16	+00:39:55.0	13.567 34	0.665 27	0.0014 ± 0.0011	−0.0010 ± 0.0008	13.53
L_92_250	00:54:37.16	+00:38:57.6	13.654 82	0.649 33	0.0000 ± 0.0011	−0.0006 ± 0.0009	12.99
L_93_317	01:54:37.73	+00:43:00.6	28.657 19	0.716 82	0.0011 ± 0.0009	−0.0020 ± 0.0009	11.42
L_93_333	01:55:05.21	+00:45:42.8	28.771 72	0.761 88	0.0010 ± 0.0026	−0.0013 ± 0.0010	12.42
L_93_424	01:55:26.36	+00:56:42.6	28.859 84	0.945 17	0.0008 ± 0.0010	−0.0024 ± 0.0011	11.34
L_94_251	02:57:46.98	+00:16:02.7	44.445 75	0.267 42	0.0039 ± 0.0010	0.0017 ± 0.0010	10.83
H_HD283807	04:44:42.60	+25:56:09.6	71.175 25	25.936 00	−0.0003 ± 0.0011	0.0006 ± 0.0008	9.96
Z_HD85471	09:59:04.94	+80:22:47.6	149.770 59	80.379 89	0.0005 ± 0.0013	0.0013 ± 0.0014	7.83
Z_HD87582	10:09:10.40	+71:41:15.5	152.291 85	71.687 63	0.0011 ± 0.0013	0.0010 ± 0.0009	7.07
Z_HD96589	11:11:00.40	+80:56:55.9	167.751 66	80.948 87	−0.0008 ± 0.0013	0.0018 ± 0.0011	7.54
Z_HD97853	11:17:09.82	+75:21:11.1	169.290 90	75.353 09	0.0001 ± 0.0007	0.0016 ± 0.0007	7.16
Z_BD+35.2256	11:30:39.95	+35:09:50.3	172.666 46	35.163 97	0.0006 ± 0.0023	0.0013 ± 0.0009	10.40
Z_BD+29.2198	11:42:56.23	+28:32:39.2	175.734 29	28.544 23	−0.0003 ± 0.0014	0.0019 ± 0.0009	10.19
Z_BD+31.2314	11:56:43.33	+30:48:45.5	179.180 56	30.812 64	−0.0003 ± 0.0011	0.0012 ± 0.0010	10.83
Z_BD+25.2439	11:56:55.10	+24:12:09.6	179.229 22	24.202 66	0.0000 ± 0.0013	0.0013 ± 0.0007	10.23
Z_BD+18.2549	11:59:04.54	+17:21:07.4	179.768 93	17.352 05	−0.0002 ± 0.0011	0.0017 ± 0.0009	10.34
Z_BD+32.2217	12:04:58.34	+31:21:06.1	181.243 09	31.351 69	−0.0002 ± 0.0008	0.0010 ± 0.0009	10.46
Z_BD+22.2446	12:11:40.13	+21:19:08.7	182.917 20	21.319 09	0.0001 ± 0.0011	0.0016 ± 0.0010	10.75
Z_BD+40.2546	12:32:44.89	+39:55:20.2	188.187 03	39.922 29	−0.0001 ± 0.0011	0.0016 ± 0.0010	10.85
Z_BD+30.2290	12:32:55.79	+29:33:52.9	188.232 47	29.564 69	0.0001 ± 0.0010	0.0020 ± 0.0009	11.39
L_104_334	12:42:20.43	−00:40:28.7	190.585 13	−0.674 54	−0.0001 ± 0.0015	0.0019 ± 0.0016	13.37
Z_BD+16.2491	13:19:08.90	+15:23:53.6	199.783 71	15.398 21	−0.0004 ± 0.0015	0.0021 ± 0.0009	11.09
Z_HD116513	13:21:49.84	+71:52:18.8	200.457 65	71.871 89	−0.0011 ± 0.0013	0.0012 ± 0.0009	7.24
L_PG1323−085B	13:25:50.65	−08:50:55.9	201.461 04	−8.848 63	0.0005 ± 0.0010	0.0016 ± 0.0005	13.21
Z_BD+31.2505	13:32:32.16	+30:49:09.5	203.133 98	30.819 31	−0.0005 ± 0.0014	0.0017 ± 0.0008	10.14
Z_BD+30.2431	13:38:24.77	+29:21:56.0	204.603 19	29.365 56	−0.0005 ± 0.0013	0.0020 ± 0.0010	10.03
Z_HD121859	13:54:53.28	+71:54:11.6	208.722 06	71.903 22	−0.0018 ± 0.0010	0.0014 ± 0.0008	7.99
L_106_700	14:40:50.94	−00:23:36.2	220.212 26	−0.393 56	−0.0040 ± 0.0009	0.0029 ± 0.0007	9.33
L_112_805	20:42:46.75	+00:16:08.1	310.694 80	0.268 91	−0.0018 ± 0.0015	0.0008 ± 0.0019	12.07
L_112_822	20:42:54.91	+00:15:01.9	310.728 81	0.250 53	−0.0033 ± 0.0015	0.0010 ± 0.0011	11.26
L_113_339	21:40:55.68	+00:27:58.1	325.231 98	0.466 13	−0.0018 ± 0.0013	−0.0009 ± 0.0010	12.10
L_113_241	21:41:09.19	+00:25:48.2	325.288 28	0.430 05	0.0006 ± 0.0021	−0.0024 ± 0.0018	13.73
B_2202+4216_129	22:02:33.40	+42:14:25.3	330.639 15	42.240 37	−0.0028 ± 0.0019	0.0022 ± 0.0013	14.10
B_2253+1608_23	22:54:11.22	+16:14:04.8	343.546 75	16.234 68	−0.0003 ± 0.0010	−0.0022 ± 0.0011	13.48
L_115_420	23:42:36.48	+01:05:58.8	355.652 02	1.099 68	−0.0017 ± 0.0010	−0.0011 ± 0.0010	11.05
High-polarization (PD > 0.5%) stars							
B_0211+1051_37	02:10:59.84	+10:48:05.7	32.749 35	10.801 58	0.0074 ± 0.0011	−0.0016 ± 0.0011	13.05
B_0211+1051_18	02:11:39.60	+10:53:15.4	32.915 01	10.887 62	0.0086 ± 0.0013	0.0004 ± 0.0015	13.50
L_94_242	02:57:21.21	+00:18:38.7	44.338 37	0.310 74	0.0050 ± 0.0013	0.0016 ± 0.0010	11.67
B_0259+0747_30	02:59:31.71	+07:44:09.4	44.882 13	7.735 94	0.0007 ± 0.0031	−0.0115 ± 0.0015	14.68
B_0303+4716_121	03:03:04.56	+47:21:25.9	45.769 02	47.357 20	−0.0089 ± 0.0037	−0.0048 ± 0.0010	14.55
H_GSC02355	03:37:45.11	+31:06:58.2	54.437 97	31.116 18	0.0348 ± 0.0025	−0.0488 ± 0.0022	12.74
L_95_330	03:54:30.75	+00:29:05.4	58.628 14	0.484 82	0.0094 ± 0.0011	−0.0018 ± 0.0009	11.16
L_95_275	03:54:44.24	+00:27:20.3	58.684 35	0.455 64	−0.0003 ± 0.0011	0.0075 ± 0.0010	12.65
L_107_599	15:39:09.46	−00:14:28.3	234.789 40	−0.241 31	−0.0067 ± 0.0011	0.0078 ± 0.0010	14.48
L_107_602	15:39:18.88	−00:15:29.0	234.828 65	−0.258 32	−0.0048 ± 0.0037	0.0083 ± 0.0015	11.82
L_PG1633+099B	16:35:33.30	+09:46:20.7	248.888 77	9.772 41	−0.0036 ± 0.0014	0.0039 ± 0.0010	12.65
L_PG1633+099D	16:35:40.90	+09:46:41.5	248.917 04	9.778 20	−0.0036 ± 0.0020	0.0038 ± 0.0013	13.54
B_1725+1152_11	17:24:47.28	+11:46:50.2	261.197 04	11.780 62	−0.0080 ± 0.0017	0.0050 ± 0.0009	13.81
B_1725+1152_24	17:24:56.26	+11:55:41.3	261.234 40	11.928 15	−0.0040 ± 0.0020	0.0046 ± 0.0008	13.86
B_1725+1152_35	17:25:15.72	+11:46:34.6	261.315 50	11.776 27	−0.0044 ± 0.0018	0.0052 ± 0.0011	12.71
B_1725+1152_113	17:25:16.51	+11:47:06.2	261.318 81	11.785 06	−0.0077 ± 0.0022	0.0055 ± 0.0008	12.79
L_109_381	17:44:12.27	−00:20:32.2	266.051 12	−0.342 45	−0.0139 ± 0.0013	0.0047 ± 0.0009	11.51
B_1751+0939_376	17:51:43.60	+09:43:51.6	267.931 68	9.731 01	−0.0077 ± 0.0030	0.0019 ± 0.0016	10.13
B_1751+0939_129	17:51:45.73	+09:40:45.3	267.940 55	9.679 24	−0.0083 ± 0.0020	0.0032 ± 0.0015	14.60
L_110_229	18:40:45.66	+00:01:49.8	280.190 26	0.030 49	0.0189 ± 0.0013	0.0150 ± 0.0018	12.53
L_110_233	18:40:52.71	+00:00:50.8	280.219 62	0.014 12	0.0240 ± 0.0017	0.0106 ± 0.0007	12.19
L_111_1965	19:37:41.56	+00:26:51.0	294.423 15	0.447 49	−0.0104 ± 0.0009	0.0064 ± 0.0010	10.70
B_1959+6508_179	19:59:12.96	+65:12:13.7	299.803 99	65.203 80	−0.0039 ± 0.0013	−0.0101 ± 0.0009	13.38
B_1959+6508_73	19:59:34.24	+65:06:19.1	299.892 67	65.105 31	−0.0007 ± 0.0018	−0.0062 ± 0.0007	12.56
B_1959+6508_104	20:00:37.89	+65:13:59.0	300.157 87	65.233 06	−0.0005 ± 0.0018	−0.0095 ± 0.0011	12.73
B_1959+6508_38	20:00:58.14	+65:07:11.9	300.242 25	65.119 96	−0.0033 ± 0.0011	−0.0155 ± 0.0008	12.50
B_2015−0137_102	20:15:04.91	−01:41:26.1	303.770 46	−1.690 81	−0.0105 ± 0.0022	−0.0030 ± 0.0016	12.84
B_2022+7611_1	20:20:52.70	+76:17:42.8	305.216 94	76.295 22	0.0062 ± 0.0010	−0.0021 ± 0.0010	12.04
B_2042+7508_28	20:41:12.89	+75:12:30.6	310.303 69	75.208 50	0.0037 ± 0.0010	0.0102 ± 0.0011	11.78
B_2340+8015_34	23:41:38.22	+80:20:16.9	355.409 26	80.338 02	0.0030 ± 0.0022	0.0119 ± 0.0016	13.73

Notes. Columns 6 and 7 contain weighted average Q/I and U/I relative Stokes parameters corrected for the instrumental polarization and EVPA zero-point. This table is available in a machine-readable format at https://doi.org/10.7910/DVN/IV9TXX.

two-sided Kolmogorov–Smirnov (KS) test. If the p-value of the KS test exceeds a given threshold, we consider the star to be non-variable and suitable for use as a standard. Otherwise, we consider it unsuitable. As mentioned earlier, if the p-value of the KS test is below the threshold, the star may indeed be variable or our uncertainty estimates of its measurements may be incorrect. We do not discriminate between these two cases. We use a threshold of $p = 0.0455$, corresponding to a 2σ confidence level, to assess the variability of stars. However, we also provide the p-values for all stars in the sample with ≥5 measurements in Table A.4. This enables the choice of a robust set of standards by filtering stars according to the p-value and opting for an alternate level of confidence. We do not perform the test for stars with fewer than five measurements, and mark them as uncertain.

We note that in the procedure described above the variability evaluation is based purely on the fractional polarization behavior, while information about the EVPA is completely ignored. However, there is a possibility that in peculiar cases the polarization vector can produce nearly perfect loops on the Q/I–U/I plane. In such a situation, the $\wp_{\rm reduced}$ remains constant, while the EVPA changes with time. For instance, binary stars with envelopes symmetric about their orbital plane can produce such polarization variability (Brown et al. 1978). In order to avoid identification of stars with this variability pattern as stable, we visually inspected distributions of measurements on the relative Stokes parameters plane for each source. We did not find any false stable stars during this inspection.

5. Results

We obtained 696 R-band and 296 SDSS r'-band measurements of 107 stars with RoboPol, which are listed in Table A.2. Additionally, for nine stars we obtained multi-band polarization measurements with ALFOSC, which are presented in Table A.3. We did not find any significant systematic difference in relative Stokes parameters between the R- and r'-bands. Therefore, we combined all measurements in these two bands and considered them together. For each star in the sample, we constructed plots of the time series data showing the evolution of the fractional polarization PD, the EVPA, and the relative Stokes parameters Q/I and U/I. These monitoring data were analyzed using the method described in Sect. 4, so that the EDF of the normalized fractional polarization given by Eq. (14) was computed for each star. Then we compared it with the distribution given by Eq. (12), which is the expected cumulative distribution of the same quantity for a stable source with the same noise level. The time series, CDF, EDF, and the distribution of measurements on the relative Stokes parameters plane for B_0017+8135_82, as an example, are shown in Fig. 6. Similar plots for all other sources in the sample are only available online[6]. As the result, we found the average polarimetric parameters for each star in the sample and classified them as stable or variable with the 2σ confidence level. These parameters and classes are listed in Table A.4. For convenience, we list only the stable stars in a separate Table 2, together with their average relative Stokes parameters and *Gaia*'s G-band magnitude. We arbitrarily place the limit between high- and low-polarization stars at PD = 0.5% in Table 2. This information, along with finding charts for all sample stars, can also be accessed online[7].

[6] https://doi.org/10.5281/zenodo.8239399
[7] https://robopol.physics.uoc.gr/standards

6. Notes on individual stars

Several stars in the sample exhibited unexpected polarization or variability. We list these sources below with a brief description of their peculiar properties.

L_PG2349+002, L_92_249, L_92_248, L_111_1969, and L_PG2213−006A were selected among the Landolt photometric standards, that is, they were expected to have stable total flux density. However, these stars exhibit significant polarization variability.

H_GSC02355 was selected as a high-polarization star from Heiles (2000), where it has PD = 5.058%. However, in our measurements, this star is variable and has a higher average polarization of 6.0%. H_HD57702 was selected as a low-polarization star from Heiles (2000), where it has a PD of 0.040 ± 0.069%. However, in our measurements, this star is 0.33% polarized.

For stars L_PG1323−085D, Z_HD153752, H_HD344776, and L_111_1969, the EDF of the reduced PD (see Sect. 4) is located entirely to the left of the theoretical CDF. It means that these stars are more stable than one would expect from the uncertainties of their PD measurements. Since we used the two-sided KS test, these stars are classified as variable. However, it is likely that the uncertainties in the relative Stokes parameters for these four sources are overestimated, and the stars are in fact stable.

7. Conclusions

We obtained 1044 polarization measurements of 107 stars using two different polarimeters. Most observations were performed in the Cousins R-band and the SDSS r'-band with the RoboPol polarimeter along a 4-yr time interval. After applying a variability analysis to these monitoring data, we selected 65 stars that have five or more measurements and do not demonstrate significant variability in linear polarization in the red bands. These stars are listed in Table 2, and they can be used as optical polarimetric standards for calibration of instrumental polarization. For 24 stars, we did not have enough data to conclude whether they are variable or stable, while the remaining 18 stars were found to exhibit significant variability in polarization.

Acknowledgements. We thank T. Pursimo and S. Armas Pérez for assistance with the NOT observations. D.B., S.K, N.M., V.P., R.S., and K.T. acknowledge support from the European Research Council (ERC) under the European Union Horizon 2020 research and innovation program under the grant agreement no. 771282. A.S. acknowledges the Polish National Science Centre grant 2017/25/B/ST9/02805. This work was supported by the NSF grant AST-2109127. The data presented here were obtained in part with ALFOSC, which is provided by the Instituto de Astrofisica de Andalucia (IAA) under a joint agreement with the University of Copenhagen and NOT.

References

Bailey, J., & Hough, J. H. 1982, PASP, 94, 618
Bastien, P., Drissen, L., Menard, F., et al. 1988, AJ, 95, 900
Bastien, P., Vernet, E., Drissen, L., et al. 2007, ASP Conf.Ser., 364, 529
Berdyugin, A., & Teerikorpi, P. 2002, A&A, 384, 1050
Berdyugin, A., Piirola, V., & Teerikorpi, P. 2014, A&A, 561, A24
Blinov, D., Kiehlmann, S., Pavlidou, V., et al. 2021, MNRAS, 501, 3715
Breus, V., Kolesnikov, S. V., & Andronov, I. L. 2021, A&A submitted, [arXiv:2112.12277]
Brown, J. C., McLean, I. S., & Emslie, A. G. 1978, A&A, 68, 415
Carrasco, L., Strom, S. E., & Strom, K. M. 1973, ApJ, 182, 95
Chentsov, E. L., Klochkova, V. G., Panchuk, V. E., Yushkin, M. V., & Nasonov, D. S. 2013, Astron. Rep., 57, 527
Cikota, A., Patat, F., Cikota, S., & Faran, T. 2017, MNRAS, 464, 4146
Clarke, D. 2009, Stellar Polarimetry (Germany: Wiley-VCH)
Clarke, D., & Naghizadeh-Khouei, J. 1994, AJ, 108, 687
Clarke, D., Naghizadeh-Khouei, J., Simmons, J. F. L., & Stewart, B. G. 1993, A&A, 269, 617

Clemens, D. P., & Tapia, S. 1990, PASP, 102, 179
Dolan, J. F., & Tapia, S. 1986, PASP, 98, 792
Gil-Hutton, R., & Benavidez, P. 2003, MNRAS, 345, 97
Heiles, C. 2000, AJ, 119, 923
Hsu, J. C., & Breger, M. 1982, ApJ, 262, 732
King, O. G., Blinov, D., Ramaprakash, A. N., et al. 2014, MNRAS, 442, 1706
Landolt, A. U. 1992, AJ, 104, 340
Maharana, S., Anche, R. M., Ramaprakash, A. N., et al. 2022, J. Astron. Telescopes Instrum. Syst., 8, 038004
Naghizadeh-Khouei, J., & Clarke, D. 1993, A&A, 274, 968
Patat, F., & Romaniello, M. 2006, PASP, 118, 146
Piirola, V., Berdyugin, A., Frisch, P. C., et al. 2020, A&A, 635, A46
Ramaprakash, A. N., Rajarshi, C. V., Das, H. K., et al. 2019, MNRAS, 485, 2355
Rice, S. O. 1945, Bell Syst. Tech. J., 24, 46
Schmidt, G. D., Elston, R., & Lupie, O. L. 1992, AJ, 104, 1563
Serkowski, K. 1958, Acta Astron., 8, 135
Simmons, J. F. L., & Stewart, B. G. 1985, A&A, 142, 100
Skalidis, R., Panopoulou, G. V., Tassis, K., et al. 2018, A&A, 616, A52
Tinbergen, J. 2007, PASP, 119, 1371
Turnshek, D. A., Bohlin, R. C., Williamson, II, R. L., et al. 1990, AJ, 99, 1243
Vaillancourt, J. E. 2006, PASP, 118, 1340
Whittet, D. C. B., Martin, P. G., Hough, J. H., et al. 1992, ApJ, 386, 562
Wiersema, K., Higgins, A. B., Covino, S., & Starling, R. L. C. 2018, PASA, 35, e012
Wiktorowicz, S. J., Słowikowska, A., Nofi, L. A., et al. 2023, ApJS, 264, 42
You, C., Zabludoff, A., Smith, P., et al. 2017, ApJ, 834, 182
Żejmo, M., Słowikowska, A., Krzeszowski, K., Reig, P., & Blinov, D. 2017, MNRAS, 464, 1294

Appendix A: Sample star information and monitoring data

Table A.1. Standard candidates sample information.

Star ID	Alt. ID	RA (J2000) h:m:s	DEC (J2000) °:′:″	Gaia ID	r' mag	G mag	Spec. typ.	Sample	N^r_{obs}	N^R_{obs}
B_0017+8135_82	-	00:15:57.61	+81:36:56.6	566773475044000896	13.40	13.42	-	B	5	10
B_0017+8135_79	-	00:16:33.82	+81:36:33.9	566773406324526592	14.05	14.07	-	B	0	1
L_92_245	SA 92-245	00:54:16.16	+00:39:54.10	2537310861359601024	-	13.53	-	L	2	11
L_92_248	SA 92-248	00:54:30.78	+00:40:17.0	2537313644497864064	14.91	14.97	-	L	2	8
L_92_249	SA 92-249	00:54:33.59	+00:41:05.4	2537313678857608448	14.11	14.15	-	L	1	9
L_92_250	SA 92-250	00:54:37.16	+00:38:57.6	2537313369619964416	12.93	12.99	-	L	2	11
L_93_317	SA 93-317	01:54:37.73	+00:43:00.6	2510809435673401472	11.42	11.42	F5	L	2	10
L_93_333	SA 93-333	01:55:05.21	+00:45:42.8	2510902962881171968		12.42	G5	L	4	12
L_93_424	SA 93-424	01:55:26.36	+00:56:42.6	2510924536502154112	11.29	11.34	G8III	L	2	10
B_0211+1051_37	Pul -3 170384	02:10:59.84	+10:48:05.7	72423941863975552	-	13.05	-	B	1	8
B_0211+1051_18	-	02:11:39.60	+10:53:15.4	72425797289881344	13.51	13.50	-	B	1	7
L_94_242	SA 94-242	02:57:21.21	+00:18:38.7	2498069944198626560	11.69	11.67	A2	L	3	9
L_94_251	SA 94-251	02:57:46.98	+00:16:02.7	2498066061548190592	-	10.83	K1III	L	3	8
B_0259+0747_30	-	02:59:31.71	+07:44:09.4	8525892335265920	14.67	14.68	-	B	1	8
B_0259+0747_22	-	02:59:40.87	+07:41:59.9	8477204585999872	14.66	14.65	-	B	2	6
B_0303+4716_121	-	03:03:04.56	+47:21:25.9	434503531895117440	14.52	14.55	-	B	0	5
H_GSC02355	GSC 02355-00137	03:37:45.11	+31:06:58.2	121211368733067392	13.02	12.74	-	H	3	7
L_95_330	SA 95-330	03:54:30.75	+00:29:05.4	3257868006962104320	11.45	11.16	-	L	3	9
L_95_275	SA 95-275	03:54:44.24	+00:27:20.3	3257866941810214400	12.81	12.65	-	L	1	5
L_95_276	SA 95-276	03:54:45.88	+00:25:54.1	3257866838731000192	13.63	13.64	-	L	0	4
H_HD283807	BD+25.728	04:44:42.6	+25:56:09.6	148254441333464576	9.95	9.96	G0	H	1	6
L_96_235	SA 96-235	04:53:18.87	−00:05:01.5	3228325297755515008	10.81	10.85	-	L	0	3
L_97_345	SA 97-345	05:57:33.18	+00:21:16.6	3218646468694578048	11.01	10.91	G8III	L	1	2
L_97_351	SA 97-351	05:57:37.28	+00:13:44.0	3218641447876998784	9.80	9.74	A0	L	0	1
H_HD255017	HD 255017	06:19:08.20	+14:38:31.0	3344737878054909312	9.36	9.35	A5Ib	H	0	2
L_98_653	HD 50188	06:52:04.95	−00:18:18.7	3113277417552594560	-	9.52	B8/9IV	L	0	1
L_98_685	SA 98-685	06:52:18.47	−00:20:19.5	3113276249321476992	-	11.84	F8	L	0	1
H_HD57702	HD 57702	07:23:24.60	+25:30:58.5	870304410193552128	-	8.87	B9	H	0	1
L_RU_152D	RU 152 D	07:30:06.7	−02:04:37.5	3061899472568519808	10.82	10.85	-	L	0	1
L_PG0918+029D	PG 0918+029 D	09:21:21.93	+02:47:28.3	3845583974466346752	11.93	11.96	-	L	1	0
Z_HD81418	BD+19.2212	09:26:02.70	+18:54:02.2	633976652229184640	8.84	8.82	A0	Z	1	1
Z_HD85471	BD+81.319	09:59:04.94	+80:22:47.6	1132568002485076352	7.78	7.83	G5	Z	4	2
Z_HD86321	BD+84.225	10:08:34.32	+83:55:06.2	1147461505958427264	5.78	5.62	K0	Z	0	1
Z_HD87582	BD+72.479	10:09:10.4	+71:41:15.5	1077571702173596928	7.06	7.07	K0	Z	3	2
L_PG1047+003	V* UY Sex	10:50:02.83	−00:00:36.1	3806303066866089216	-	13.42	sdO9VIIHe6	L	1	0
L_PG1047+003B	PG 1047+003 B	10:50:07.92	−00:02:04.6	3806302787692664832	14.55	14.58	-	L	1	0
L_PG1047+003C	PG 1047+003 C	10:50:13.68	−00:00:32.7	3806303200009524480	-	12.31	-	L	1	0
L_G163_50	WD 1105-048	11:07:59.95	−05:09:26.10	3788194488314248832	13.24	13.09	DA3	L	2	0
L_G163_51	L 970-27	11:08:06.54	−05:13:47.9	3788190605663811840	–	11.47	M3V	L	2	1
Z_HD96589	BD+81.362	11:11:00.40	+80:56:55.9	1133527773057098752	7.51	7.54	G0	Z	4	1
Z_HD97853	BD+76.421	11:17:09.82	+75:21:11.1	1079936717325036160	7.14	7.16	K0	Z	3	3
Z_BD+35.2256	BD+35.2256	11:30:39.95	+35:09:50.3	759519993695325696	10.41	10.40	F2	Z	3	6
Z_BD+29.2198	BD+29.2198	11:42:56.23	+28:32:39.2	4018335981542938112	-	10.19	A2	Z	4	6

Table A.1. continued

Z_BD+31.2314	BD+31.2314	11:56:43.33	+30:48:45.5	4026504219066025600	-	10.83	kA3hA7:m	Z	5	3
Z_BD+25.2439	BD+25.2439	11:56:55.1	+24:12:09.6	4004411731929387904	-	10.23	F5	Z	3	4
Z_BD+18.2549	BD+18.2549	11:59:04.54	+17:21:07.4	3926601527414968704	10.33	10.34	G0	Z	3	4
Z_BD+32.2217	BD+32.2217	12:04:58.34	+31:21:06.1	4026404644544171520	-	10.46	kA4hA7VmF2	Z	4	4
Z_BD+22.2446	BD+22.2446	12:11:40.13	+21:19:08.7	3951825148789721472	-	10.75	-	Z	3	4
Z_BD+40.2546	BD+40.2546	12:32:44.89	+39:55:20.2	1533606794177007104	10.85	10.85	F6	Z	3	8
Z_BD+30.2290	BD+30.2290	12:32:55.79	+29:33:52.9	4011002135906720768	11.41	11.39	A2	Z	4	4
L_104_334	SA 104-334	12:42:20.43	−00:40:28.7	3683802417670914688	13.36	13.37	–	L	5	3
Z_BD+39.2611	* 15 CVn	13:09:42.3	+38:32:01.10	1523140405554059008	6.44	6.29	B7III	Z	0	1
Z_BD+16.2491	BD+16.2491	13:19:08.9	+15:23:53.6	3744299780814144896	11.06	11.09	-	Z	5	3
Z_HD116513	BD+72.613	13:21:49.84	+71:52:18.8	1687792271812816384	7.20	7.24	K2	Z	5	8
L_PG1323−085B	PG 1323-086 B	13:25:50.65	−08:50:55.9	3624196212997860992	13.18	13.21	-	L	3	3
L_PG1323−085C	PG 1323-086 C	13:25:50.22	−08:48:38.0	3624199374093791616	13.79	13.83	-	L	2	0
L_PG1323−085D	PG 1323-086 D	13:26:05.25	−08:50:36.8	3624196109918646016	11.91	11.93	-	L	3	3
Z_BD+31.2505	BD+31.2505	13:32:32.16	+30:49:09.5	1468318824514203264	10.20	10.14	-	Z	5	6
Z_BD+35.2465	BD+35.2465	13:35:23.76	+35:13:39.1	1471664741475242112	10.86	10.82	-	Z	0	4
Z_BD+30.2431	Feige 86	13:38:24.77	+29:21:56.0	1455929733649174528	10.20	10.03	B5Vp	Z	3	4
Z_HD120010	BD+11.2600	13:46:37.63	+10:50:26.2	3726354449674413696	8.26	8.30	K2	Z	0	2
Z_HD121859	BD+72.631	13:54:53.28	+71:54:11.6	1687308933373463808	7.96	7.99	K2	Z	4	9
L_106_700	BD+00.3222	14:40:50.94	−00:23:36.2	3651584807127464960	9.33	9.33	K0III	L	2	9
Z_HD138733	BD+71.733	15:28:51.17	+70:40:52.5	1695728233208611328	8.31	8.35	K0	Z	5	10
L_107_599	SA 107-599	15:39:09.46	−00:14:28.3	4416475498513533952	14.45	14.48	-	L	3	5
L_107_602	SA 107-602	15:39:18.88	−00:15:29.0	4416474639520070144	-	11.82	F8	L	3	7
L_PG1633+099B	PG 1633+099 B	16:35:33.30	+09:46:20.7	4446607820836297344	12.60	12.65	-	L	3	10
L_PG1633+099D	PG 1633+099 D	16:35:40.9	+09:46:41.5	4446607752116815232	13.53	13.54	-	L	5	9
Z_HD153752	BD+74.690	16:53:38.18	+74:17:30.1	1656269376524601472	7.66	7.64	F0	Z	5	11
B_1725+1152_11	-	17:24:47.28	+11:46:50.2	4540367777239708416	13.80	13.81	-	B	2	7
B_1725+1152_24	-	17:24:56.26	+11:55:41.3	4540374516046715648	13.82	13.86	-	B	3	8
B_1725+1152_35	-	17:25:15.72	+11:46:34.6	4492329534405398016	12.67	12.71	-	B	5	10
B_1725+1152_113	-	17:25:16.51	+11:47:06.2	4492331011874148480	12.78	12.79	-	B	3	9
L_109_71	SA 109-71	17:44:06.79	−00:24:58.9	4371937237413220096	11.46	11.43	A0	L	0	3
L_109_381	SA 109-381	17:44:12.27	−00:20:32.2	4371985993881977856	11.49	11.51	F2	L	5	10
B_1751+0939_376	-	17:51:43.60	+09:43:51.6	4488790412635906176	11.84	10.13	-	B	4	10
B_1751+0939_129	-	17:51:45.73	+09:40:45.3	4488787973094456448	14.58	14.60	-	B	3	10
B_1751+0939_204	-	17:51:48.7	+09:41:44.8	4488789484922948352	14.93	14.24	-	B	2	9
L_110_229	SA 110-229	18:40:45.66	+00:01:49.8	4272464794108661760	12.89	12.53	-	L	6	13
L_110_233	SA 110-233	18:40:52.71	+00:00:50.8	4272452974358663680	12.31	12.19	-	L	4	10
L_111_1965	SA 111-1965	19:37:41.56	+00:26:50.10	4239473470987190016	10.83	10.70	K0	L	6	11
L_111_1969	BD+00.4260	19:37:43.28	+00:25:48.5	4239285763738341632	9.69	9.28	M5III	L	6	13
H_HD344776	BD+23.3745	19:42:49.62	+23:27:47.9	2020105333313222144	8.54	8.53	B0.5Ib	H	4	12
B_1959+6508_179	-	19:59:12.96	+65:12:13.7	2247538007835538176	13.35	13.38	-	B	3	7
B_1959+6508_73	-	19:59:34.24	+65:06:19.1	2247536152409628032	12.68	12.56	-	B	5	9
B_1959+6508_108	-	20:00:21.39	+65:13:59.5	2247560822701907200	14.36	14.39	-	B	3	9
B_1959+6508_104	-	20:00:37.89	+65:13:59.0	2247550583499874304	12.76	12.73	-	B	4	10

Table A.1. continued

B_1959+6508_38	-	20:00:58.14	+65:07:11.9	2247547525483073792	12.51	12.50	-	B	4	9
B_2015−0137_102	-	20:15:04.91	−01:41:26.1	4223920844642460032	12.83	12.84	-	B	4	14
B_2022+7611_1	-	20:20:52.7	+76:17:42.8	2290191431129629952	12.05	12.04	-	B	5	9
B_2042+7508_28	-	20:41:12.89	+75:12:30.6	2277833706411214464	11.83	11.78	-	B	5	8
L_112_805	SA 112-805	20:42:46.75	+00:16:08.1	4228196566186425216	12.15	12.07	A0	L	5	13
L_112_822	SA 112-822	20:42:54.91	+00:15:01.9	4228184578933327872	11.22	11.26	G8III	L	3	13
B_2042+7508_17	-	20:42:55.65	+75:09:42.5	2277830961927902336	14.89	14.89	-	B	4	7
L_113_339	SA 113-339	21:40:55.68	+00:27:58.1	2687421308383972992	12.09	12.10	F8	L	0	8
L_113_241	SA 113-241	21:41:09.19	+00:25:48.2	2687420170216933888	13.77	13.73	-	L	3	10
B_2202+4216_25	-	22:02:17.6	+42:21:06.0	1960081928389196800	12.82	12.69	-	B	4	10
B_2202+4216_129	-	22:02:33.40	+42:14:25.3	1960065779311967488	14.08	14.10	-	B	5	13
B_2202+4216_239	-	22:02:54.47	+42:10:24.9	1960061823644122112	15.05	15.03	-	B	4	9
H_BD+62.2078	BD+62.2078	22:25:33.57	+63:25:02.6	2205414029452444800	9.34	9.25	O7V((f))z	H	5	12
L_PG2213−006A	PG 2213-006 A	22:16:23.21	−00:21:27.10	2678666889428745088	13.98	13.99	-	L	4	9
B_2253+1608_23	-	22:54:11.22	+16:14:04.8	2828722296448918144	-	13.48	-	B	3	8
B_2340+8015_34	-	23:41:38.22	+80:20:16.9	2283216988357240064	13.74	13.73	-	B	4	7
B_2340+8015_109	-	23:42:21.63	+80:11:05.0	2283199499250447488	13.65	13.68	-	B	0	4
B_2340+8015_99	-	23:42:26.8	+80:12:06.3	2283211353360181376	13.34	13.36	-	B	5	10
L_115_420	SA 115-420	23:42:36.48	+01:05:58.8	2646050087444966272	-	11.05	F5	L	2	13
L_PG2349+002	-	23:51:53.23	+00:28:17.7	2642341469085008000	-	13.26	sdB2VIIHe0	L	3	3

Table A.2. Polarimetric monitoring data.

Star ID	JD	Band	$q = Q/I$	$u = U/I$	PD %	EVPA °
B_0017+8135_82	2457962.42898	R	−0.0066 ± 0.0014	0.0012 ± 0.0012	0.7 ± 0.1	85 ± 6
B_0017+8135_82	2457987.52889	R	−0.0064 ± 0.0012	0.0017 ± 0.0011	0.7 ± 0.1	83 ± 5
B_0017+8135_82	2458015.46020	R	−0.0080 ± 0.0012	0.0018 ± 0.0010	0.8 ± 0.1	84 ± 4
			...			

This table gives only the first three rows of the entire dataset, which can be accessed at https://doi.org/10.7910/DVN/IV9TXX.

Table A.3. Multiband single epoch measurements with ALFOSC/NOT.

Star ID	Alt. ID	Band	q	σ_q	u	σ_u	PD %	σ_{PD} %	EVPA °	σ_{EVPA} °
B_1959+6508_38	-	B	−0.0009	0.0016	−0.0181	0.0017	1.8	0.2	−47	3
		V	−0.0016	0.0009	−0.0186	0.0011	1.9	0.1	−48	2
RA=20h00m58.14s		R	−0.0061	0.0009	−0.0172	0.0012	1.8	0.1	−55	2
DEC=+65d07m11.9s		g	−0.0016	0.0013	−0.0196	0.0014	2.0	0.1	−47	2
		r	−0.0039	0.0009	−0.0175	0.0011	1.8	0.1	−51	2
		i	−0.0048	0.0008	−0.0160	0.0011	1.7	0.1	−53	2
B_2015−0137_102	-	B	−0.0108	0.0009	−0.0067	0.0011	1.27	0.10	−74	2
		V	−0.0119	0.0010	−0.0061	0.0011	1.34	0.10	−77	2
RA=20h15m04.91s		R	−0.0114	0.0009	−0.0049	0.0011	1.23	0.09	−78	2
DEC=−01d41m26.1s		g	−0.0096	0.0007	−0.0087	0.0009	1.29	0.08	−69	2
		r	−0.0116	0.0008	−0.0062	0.0011	1.31	0.09	−76	2
		i	−0.0105	0.0009	−0.0047	0.0012	1.15	0.10	−78	2
B_2042+7508_17	-	B	−0.0024	0.0016	0.0097	0.0018	1.0	0.2	52	5
		V	−0.0017	0.0012	0.0102	0.0013	1.0	0.1	50	4
RA=20h42m55.65s		R	−0.0024	0.0011	0.0101	0.0013	1.0	0.1	51	4
DEC=+75d09m42.5s		g	0.0001	0.0042	0.0070	0.0038	0.7	0.4	45	19
		r	−0.0013	0.0013	0.0093	0.0013	0.9	0.1	49	4
		i	−0.0011	0.0009	0.0078	0.0012	0.8	0.1	49	4
H_HD344776	BD+23.3745	U	0.0287	0.0014	0.0426	0.0015	5.14	0.15	28.0	0.8
		B	0.0292	0.0006	0.0531	0.0008	6.06	0.07	30.6	0.3
RA=19h42m49.62s		V	0.0374	0.0006	0.0527	0.0008	6.46	0.07	27.3	0.3
DEC=+23d27m47.9s		R	0.0424	0.0006	0.0455	0.0009	6.22	0.07	23.5	0.3
		g	0.0321	0.0005	0.0547	0.0008	6.34	0.07	29.8	0.3
L_93_333	SA 93−333	B	−0.0001	0.0011	−0.0046	0.0013	0.46	0.13	−46	8
		V	−0.0001	0.0010	−0.0026	0.0011	0.26	0.11	−45	14
RA=01h55m05.21s		R	−0.0002	0.0007	−0.0036	0.0010	0.36	0.10	−47	8
DEC=+00d45m42.8s		g	0.0012	0.0007	−0.0027	0.0009	0.30	0.09	−33	9
		r	0.0008	0.0007	−0.0030	0.0010	0.31	0.09	−38	10
		i	−0.0014	0.0007	−0.0040	0.0010	0.43	0.10	−55	7
L_94_242	SA 94−242	U	0.0044	0.0031	0.0024	0.0031	0.50	0.31	14	23
		B	0.0036	0.0007	0.0017	0.0010	0.40	0.08	13	6
RA=02h57m21.21s		V	0.0043	0.0007	0.0006	0.0009	0.43	0.07	4	5
DEC=+00d18m38.7s		R	0.0044	0.0007	−0.0009	0.0010	0.44	0.07	−6	5
		r	0.0047	0.0006	0.0004	0.0009	0.47	0.06	3	4
		i	0.0040	0.0007	−0.0021	0.0010	0.45	0.08	−14	5
L_110_229	SA 110−229	B	0.0133	0.0010	0.0172	0.0012	2.17	0.11	26.1	1.4
		V	0.0188	0.0011	0.0160	0.0012	2.47	0.11	20.2	1.3
RA=18h40m45.66s		R	0.0192	0.0010	0.0156	0.0012	2.47	0.11	19.5	1.2
DEC=+00d01m49.8s		g	0.0164	0.0007	0.0169	0.0009	2.35	0.08	22.9	1.0
		r	0.0183	0.0010	0.0153	0.0012	2.39	0.11	20.0	1.3
		i	0.0174	0.0008	0.0120	0.0011	2.11	0.09	17.3	1.2
L_111_1965	SA 111−1965	B	−0.0105	0.0010	0.0008	0.0012	1.06	0.10	87.9	3
		V	−0.0113	0.0008	0.0040	0.0010	1.20	0.08	80.2	2
RA=19h37m41.56s		R	−0.0119	0.0007	0.0046	0.0010	1.27	0.08	79.5	2
DEC=+00d26m50.10s		g	−0.0106	0.0007	0.0026	0.0010	1.09	0.08	83.2	2
		r	−0.0098	0.0007	0.0041	0.0010	1.06	0.08	78.6	2
		i	−0.0087	0.0006	0.0038	0.0009	0.95	0.07	78.1	2
L_112_805	SA 112−805	B	−0.0016	0.0009	−0.0004	0.0011	0.16	0.09	−83	20
		V	−0.0026	0.0010	−0.0005	0.0012	0.27	0.10	−85	12
RA=20h42m46.75s		R	−0.0026	0.0014	−0.0005	0.0015	0.27	0.14	−84	18
DEC=+00d16m08.1s		g	−0.0019	0.0007	−0.0003	0.0010	0.19	0.07	−85	12
		r	−0.0035	0.0013	0.0010	0.0014	0.36	0.13	82	11
		i	−0.0027	0.0014	−0.0006	0.0016	0.28	0.14	−84	18

Table A.4. Average polarization parameters of the sample stars.

Star ID	N meas.	PD	σPD	EVPA	σ EVPA	q	σ_q	u	σ_u	Var. flag	p-value
		%	%	°	°						
B_0017+8135_82	15	0.671	0.031	79.7	1.3	-0.00628	0.00174	0.00236	0.00220	V	0.0032
B_0017+8135_79	1	0.461	0.119	84.8	7.8	-0.00454	0.00120	0.00083	0.00098	UN	-
L_92_245	13	0.173	0.030	-16.9	5.1	0.00144	0.00105	-0.00096	0.00085	NV	0.5008
L_92_248	10	0.412	0.047	-12.8	3.3	0.00372	0.00377	-0.00177	0.00175	V	0.0174
L_92_249	10	0.403	0.040	-17.3	2.9	0.00331	0.00368	-0.00229	0.00173	V	0.0005
L_92_250	13	0.055	0.030	-46.0	19.1	-0.00002	0.00107	-0.00055	0.00092	NV	0.2647
L_93_317	12	0.230	0.031	-31.0	3.9	0.00108	0.00095	-0.00203	0.00092	NV	0.6470
L_93_333	16	0.167	0.026	-26.4	4.6	0.00101	0.00262	-0.00133	0.00102	NV	0.3953
L_93_424	12	0.253	0.030	-35.7	3.5	0.00081	0.00096	-0.00240	0.00107	NV	0.5936
B_0211+1051_37	9	0.761	0.040	-6.1	1.5	0.00743	0.00118	-0.00162	0.00116	NV	0.9640
B_0211+1051_18	8	0.857	0.044	1.4	1.5	0.00856	0.00135	0.00042	0.00146	NV	0.7017
L_94_242	12	0.530	0.033	8.9	1.8	0.00505	0.00129	0.00161	0.00095	NV	0.9261
L_94_251	11	0.425	0.033	12.0	2.2	0.00388	0.00096	0.00173	0.00099	NV	0.8108
B_0259+0747_30	9	1.153	0.046	-43.4	1.1	0.00065	0.00311	-0.01151	0.00148	NV	0.1567
B_0259+0747_22	8	0.826	0.051	-68.0	1.8	-0.00594	0.00485	-0.00575	0.00154	V	0.0017
B_0303+4716_121	5	1.013	0.054	-75.8	1.5	-0.00892	0.00370	-0.00481	0.00101	NV	0.3281
H_GSC02355	10	5.998	0.042	-27.2	0.2	0.03484	0.00247	-0.04883	0.00217	NV	0.1163
L_95_330	12	0.962	0.034	-5.5	1.0	0.00944	0.00111	-0.00184	0.00089	NV	0.7842
L_95_275	6	0.752	0.044	46.2	1.7	-0.00032	0.00121	0.00751	0.00104	NV	0.8362
L_95_276	4	0.204	0.051	44.8	7.5	0.00001	0.00234	0.00204	0.00416	UN	-
H_HD283807	7	0.066	0.040	59.5	22.6	-0.00032	0.00116	0.00058	0.00084	NV	0.2401
L_96_235	3	0.150	0.060	-19.9	12.7	0.00115	0.00009	-0.00096	0.00066	UN	-
L_97_345	3	1.411	0.064	-0.5	1.3	0.01411	0.00106	-0.00024	0.00020	UN	-
L_97_351	1	1.013	0.094	-35.1	2.7	0.00343	0.00114	-0.00953	0.00091	UN	-
H_HD255017	2	0.237	0.071	29.8	9.2	0.00120	0.00031	0.00205	0.00073	UN	-
L_98_653	1	0.439	0.112	75.4	7.6	-0.00384	0.00116	0.00214	0.00098	UN	-
L_98_685	1	0.201	0.114	-9.5	20.6	0.00190	0.00116	-0.00066	0.00095	UN	-
H_HD57702	1	0.332	0.115	1.1	10.8	0.00332	0.00115	0.00013	0.00095	UN	-
L_RU_152D	1	0.297	0.113	2.8	12.1	0.00295	0.00113	0.00029	0.00092	UN	-
L_PG0918+029D	1	0.372	0.226	89.1	22.8	-0.00372	0.00226	0.00011	0.00231	UN	-
Z_HD81418	2	0.140	0.086	68.4	23.1	-0.00102	0.00028	0.00096	0.00134	UN	-
Z_HD85471	6	0.141	0.047	35.4	10.2	0.00046	0.00129	0.00134	0.00141	NV	0.7495
Z_HD86321	1	0.132	0.110	-86.7	61.4	-0.00131	0.00110	-0.00015	0.00089	UN	-
Z_HD87582	5	0.147	0.054	21.6	11.6	0.00107	0.00132	0.00101	0.00094	NV	0.9888
L_PG1047+003	1	0.209	0.136	48.2	25.4	-0.00023	0.00152	0.00207	0.00136	UN	-
L_PG1047+003B	1	0.159	0.155	3.7	61.4	0.00157	0.00155	0.00020	0.00139	UN	-
L_PG1047+003C	1	0.190	0.145	75.0	61.4	-0.00164	0.00148	0.00095	0.00133	UN	-
L_G163_50	2	0.146	0.123	44.8	61.4	0.00001	0.00193	0.00146	0.00132	UN	-
L_G163_51	3	0.192	0.080	28.8	13.7	0.00103	0.00146	0.00162	0.00007	UN	-
Z_HD96589	5	0.193	0.051	56.9	8.0	-0.00078	0.00134	0.00177	0.00118	NV	0.9093
Z_HD97853	6	0.159	0.043	42.7	8.3	0.00013	0.00070	0.00158	0.00074	NV	0.0839
Z_BD+35.2256	9	0.146	0.039	32.4	8.1	0.00062	0.00242	0.00133	0.00088	NV	0.4036
Z_BD+29.2198	10	0.192	0.033	48.8	5.1	-0.00025	0.00143	0.00190	0.00087	NV	0.4883
Z_BD+31.2314	8	0.122	0.040	51.3	10.3	-0.00026	0.00108	0.00119	0.00104	NV	0.3385
Z_BD+25.2439	7	0.131	0.042	44.8	9.8	0.00001	0.00131	0.00131	0.00071	NV	0.7856
Z_BD+18.2549	7	0.170	0.042	48.5	7.5	-0.00021	0.00121	0.00168	0.00091	NV	0.4239
Z_BD+32.2217	8	0.104	0.040	51.7	12.3	-0.00024	0.00077	0.00101	0.00090	NV	0.1073
Z_BD+22.2446	7	0.159	0.042	43.9	8.0	0.00006	0.00120	0.00159	0.00097	NV	0.2292
Z_BD+40.2546	11	0.164	0.032	47.3	5.8	-0.00013	0.00107	0.00164	0.00097	NV	0.5166
Z_BD+30.2290	8	0.203	0.039	43.7	5.7	0.00009	0.00097	0.00202	0.00094	NV	0.6699
L_104_334	8	0.187	0.042	45.9	6.6	-0.00006	0.00150	0.00187	0.00161	NV	0.0743
Z_BD+39.2611	1	0.055	0.112	-88.3	61.4	-0.00055	0.00112	-0.00003	0.00090	UN	-
Z_BD+16.2491	8	0.212	0.039	51.1	5.4	-0.00045	0.00151	0.00207	0.00085	NV	0.5325
Z_HD116513	13	0.167	0.030	66.3	5.3	-0.00113	0.00128	0.00123	0.00091	NV	0.7017
L_PG1323-085C	2	0.275	0.097	64.0	11.1	-0.00169	0.00062	0.00217	0.00098	UN	-
L_PG1323-085B	6	0.173	0.047	35.8	8.3	0.00054	0.00102	0.00164	0.00060	NV	0.0854
L_PG1323-085D	6	0.142	0.045	59.0	9.6	-0.00067	0.00065	0.00126	0.00039	V	0.0049
Z_BD+31.2505	11	0.179	0.033	52.6	5.4	-0.00047	0.00145	0.00173	0.00084	NV	0.9933
Z_BD+35.2465	4	0.190	0.053	56.7	8.5	-0.00075	0.00057	0.00174	0.00080	UN	-
Z_BD+30.2431	7	0.208	0.043	51.6	6.1	-0.00048	0.00126	0.00203	0.00100	NV	0.7369
Z_HD120010	2	0.171	0.071	57.5	13.4	-0.00073	0.00003	0.00155	0.00010	UN	-
Z_HD121859	13	0.226	0.031	71.5	3.9	-0.00181	0.00097	0.00136	0.00078	NV	0.1764
L_106_700	11	0.494	0.033	72.4	1.9	-0.00404	0.00090	0.00285	0.00067	NV	0.1658
Z_HD138733	15	0.068	0.030	89.5	14.7	-0.00068	0.00070	0.00001	0.00091	V	0.0129
L_107_599	8	1.031	0.045	65.3	1.3	-0.00670	0.00123	0.00784	0.00102	NV	0.6894
L_107_602	10	0.963	0.040	60.1	1.2	-0.00483	0.00374	0.00833	0.00154	NV	0.8954

Table A.4. continued

L_PG1633+099B	13	0.532	0.032	66.1	1.8	-0.00357	0.00140	0.00394	0.00097	NV	0.8427
L_PG1633+099D	14	0.523	0.038	66.6	2.1	-0.00358	0.00199	0.00381	0.00126	NV	0.8657
Z_HD153752	16	0.107	0.027	61.4	7.6	-0.00058	0.00102	0.00090	0.00046	V	0.0222
B_1725+1152_11	9	0.938	0.041	74.1	1.3	-0.00797	0.00169	0.00495	0.00087	NV	0.8484
B_1725+1152_24	11	0.610	0.036	65.2	1.7	-0.00396	0.00195	0.00464	0.00079	NV	0.3462
B_1725+1152_35	15	0.681	0.037	65.2	1.6	-0.00442	0.00183	0.00518	0.00111	NV	0.9634
B_1725+1152_113	12	0.942	0.034	72.2	1.0	-0.00767	0.00220	0.00547	0.00076	NV	0.4971
L_109_71	3	1.443	0.065	85.2	1.3	-0.01422	0.00032	0.00243	0.00058	UN	-
L_109_381	15	1.470	0.030	80.7	0.6	-0.01392	0.00127	0.00471	0.00089	NV	0.3730
B_1751+0939_376	14	0.795	0.033	83.1	1.2	-0.00772	0.00296	0.00189	0.00163	NV	0.6864
B_1751+0939_129	13	0.887	0.040	79.3	1.3	-0.00826	0.00203	0.00323	0.00145	NV	0.4327
B_1751+0939_204	11	0.147	0.045	-19.3	9.4	0.00115	0.00418	-0.00092	0.00141	V	0.0147
L_110_229	19	2.408	0.029	19.2	0.3	0.01887	0.00132	0.01495	0.00176	NV	0.3421
L_110_233	14	2.620	0.033	12.0	0.4	0.02395	0.00167	0.01062	0.00070	NV	0.1857
L_111_1965	17	1.216	0.028	74.2	0.7	-0.01035	0.00094	0.00637	0.00099	NV	0.7499
L_111_1969	19	1.229	0.028	75.9	0.6	-0.01082	0.00110	0.00583	0.00082	V	0.0219
H_HD344776	16	6.101	0.034	25.3	0.2	0.03880	0.00095	0.04709	0.00074	V	0.0006
B_1959+6508_179	10	1.087	0.035	-55.6	0.9	-0.00392	0.00127	-0.01014	0.00087	NV	0.3940
B_1959+6508_73	14	0.623	0.029	-48.4	1.3	-0.00073	0.00177	-0.00619	0.00069	NV	0.7553
B_1959+6508_108	12	0.955	0.033	-53.8	1.0	-0.00288	0.00325	-0.00911	0.00189	V	0.0004
B_1959+6508_104	14	0.953	0.029	-46.6	0.9	-0.00054	0.00181	-0.00951	0.00116	NV	0.8586
B_1959+6508_38	13	1.587	0.030	-51.1	0.5	-0.00333	0.00118	-0.01552	0.00083	NV	0.4246
B_2015-0137_102	18	1.097	0.029	-82.0	0.7	-0.01054	0.00218	-0.00303	0.00158	NV	0.3969
B_2022+7611_1	14	0.651	0.031	-9.2	1.4	0.00618	0.00098	-0.00205	0.00095	NV	0.8763
B_2042+7508_28	13	1.088	0.030	34.9	0.8	0.00374	0.00102	0.01022	0.00109	NV	0.2030
L_112_805	18	0.196	0.030	78.6	4.5	-0.00180	0.00154	0.00076	0.00195	NV	0.1500
L_112_822	16	0.349	0.029	81.7	2.4	-0.00334	0.00147	0.00100	0.00124	NV	0.1203
B_2042+7508_17	11	0.995	0.039	44.2	1.1	0.00028	0.00390	0.00995	0.00200	V	1.4×10^{-5}
L_113_339	8	0.198	0.040	-76.4	5.9	-0.00176	0.00130	-0.00090	0.00096	NV	0.5852
L_113_241	13	0.249	0.038	-38.0	4.4	0.00060	0.00208	-0.00242	0.00183	NV	0.1112
B_2202+4216_25	14	1.063	0.030	64.5	0.8	-0.00670	0.00195	0.00826	0.00086	V	0.0348
B_2202+4216_129	18	0.359	0.032	71.1	2.5	-0.00283	0.00195	0.00220	0.00126	NV	0.6288
B_2202+4216_239	13	1.116	0.039	-70.2	1.0	-0.00860	0.00215	-0.00711	0.00178	V	0.0206
L_PG2213-006A	13	0.379	0.040	-22.6	3.1	0.00267	0.00409	-0.00269	0.00208	V	0.0181
H_BD+62.2078	17	7.471	0.036	72.7	0.1	-0.06156	0.00126	0.04233	0.00102	V	0.0365
B_2253+1608_23	11	0.224	0.039	-48.4	5.1	-0.00026	0.00100	-0.00222	0.00110	NV	0.1920
B_2340+8015_34	11	1.229	0.037	37.9	0.9	0.00301	0.00225	0.01192	0.00158	NV	0.1264
B_2340+8015_109	4	1.273	0.057	18.7	1.3	0.01011	0.00051	0.00773	0.00105	UN	-
B_2340+8015_99	15	1.147	0.029	13.3	0.7	0.01025	0.00285	0.00513	0.00194	V	0.0006
L_115_420	15	0.199	0.028	-73.2	4.2	-0.00165	0.00102	-0.00110	0.00104	NV	0.7984
L_PG2349+002	6	0.798	0.059	-26.0	2.1	0.00490	0.00541	-0.00629	0.00479	V	1.7×10^{-9}

Notes. Var. flag column is given for 2σ S.L. and has the following meaning: "NV" stands for non-variable; "V" for variable; "UN" for uncertain. This table is available in a machine-readable format at https://doi.org/10.7910/DVN/IV9TXX.